Fabrication and characterization of transparent conducting titanium-zinc oxide nanostructured thin films*

LU Zhou (陆轴)[1], **LONG Lu** (龙路)[1], **ZHONG Zhi-you** (钟志有)[1,2]**, **HOU Jin** (侯金)[1,2], **YANG Chun-yong** (杨春勇)[1,2], **GU Jin-hua** (顾锦华)[3], **and LONG Hao** (龙浩)[1]

1. College of Electronic Information Engineering, South-Central University for Nationalities, Wuhan 430074, China

2. Hubei Key Laboratory of Intelligent Wireless Communications, South-Central University for Nationalities, Wuhan 430074, China

3. Center of Experiment Teaching, South-Central University for Nationalities, Wuhan 430074, China

(Received 9 December 2015)

Nano transparent conducting titanium-zinc oxide (Ti-ZnO) thin films were prepared on glass substrates by radio frequency (RF) magnetron sputtering technique. The deposited films are characterized by X-ray diffraction (XRD), four-probe meter and UV-visible spectrophotometer. The effects of Ti-doping content on the structural, optical and electrical properties of the films are investigated. The XRD results show that the obtained films are polycrystalline with a hexagonal wurtzite structure and preferentially oriented in the (002) crystallographic direction. The structural and optoelectronic characteristics of the deposited films are subjected to the Ti-doping content. The Ti-ZnO sample fabricated with the Ti-doping content of 3% (weight percentage) possesses the best crystallinity and optoelectronic performance, with the highest degree of preferred (002) orientation of 99.87%, the largest crystallite size of 83.2 nm, the minimum lattice strain of 6.263×10^{-4}, the highest average visible transmittance of 88.8%, the lowest resistivity of 1.18×10^{-3} Ω·cm and the maximum figure of merit (*FOM*) of 7.08×10^{3} $\Omega^{-1}\cdot cm^{-1}$. Furthermore, the optical bandgaps of the films are evaluated by extrapolation method and observed to be an increasing tendency with the increase of the Ti-doping content.

Document code: A **Article ID:** 1673-1905(2016)02-0128-4

DOI 10.1007/s11801-016-5256-6

Transparent conducting oxide (TCO) thin films have been widely used as transparent electrodes in optoelectronic devices, such as photovoltaic solar cells[1-3], organic electroluminescent diodes[4,5], flat panel displays[6], thin film transistors[7] and chemical sensors[8], due to their excellent electrical and optical properties. ZnO thin films can be deposited at relatively low temperatures resulting in polycrystal structure and can be doped with additional elements, such as boron (B), aluminum (Al), gallium (Ga) and indium (In), to improve the electrical resistivity. Moreover, they are also chemically stable in hydrogen plasma processes that are commonly used for the production of photovoltaic solar cells[9]. Many techniques have been developed to prepare the doped ZnO TCO thin films, such as magnetron sputtering[6,10,11], atomic layer deposition[1], sol-gel process[12,13], chemical spray[14], pulsed laser deposition[15], etc. Among these deposition techniques, the magnetron sputtering is regarded as an effective method for preparing TCO thin films.

In this work, the ZnO and titanium-zinc oxide (Ti-ZnO) nanostructured thin films were deposited on glass substrates by radio frequency (RF) magnetron sputtering technique in an argon environment. The effects of Ti-doping content on the structural, optical and electrical properties of the thin films are investigated by means of X-ray diffraction (XRD), UV-visible spectrophotometer and four-point probe, respectively.

The $TiZnO_3$ ceramic sputtering targets were prepared with the mixed powder of ZnO (99.99% in purity) and TiO_2 (99.99% in purity), containing 0—5% (weight percentage, the same below) TiO_2, respectively. Glass substrates were dipped into acetone and cleaned with ultrasonic washer for 15 min, and then cleaned by alcohol with ultrasonic washer for 15 min, then dried. The sputtering chamber was evacuated to a base pressure below 5.2×10^{-4} Pa before argon gas. After vacuum pumping, the sputtering argon gas with a purity of 99.99% was introduced into the chamber and controlled by the standard mass flow controllers. Before the thin

* This work has been supported by the National Natural Science Foundation of China (Nos.11504435 and 11504436), and the Natural Science Foundation of Hubei (Nos.2013CFA052, 2014CFA051 and 2015CFB364).

** E-mail: zyzhongzy@163.com

4films deposition, pre-sputtering was conducted for 12 min to attain stability and to remove impurities. The deposition parameters for growing ZnO and Ti-ZnO samples are as follows: the target to substrate distance is 70 mm, the substrate temperature is 550 K, the argon pressure is 0.5 Pa, and the RF sputtering power is 180 W.

The structural, optical and electrical properties of the deposited thin films are characterized by various techniques. The crystallographic and phase structures are determined by XRD. A D8-Advance diffractometer with Cu Kα source and Ni filter is used for the XRD measurement. The electrical properties are evaluated with an SZ-82 four-probe meter. The optical transmission measurements are carried out with a TU-1901 double-beam UV-visible spectrophotometer. The spectral region used in this work is 200—800 nm.

Fig.1 shows XRD patterns of ZnO and Ti-ZnO samples with different Ti-doping contents, and the XRD analysis results are summarized in Tab.1. Note that all the samples exhibit a dominant (002) peak with slight (100) and (110) peaks in the displayed 2θ region. Neither metallic titanium and zinc characteristic peaks nor titanium oxide peak can be observed from the XRD patterns, which implies that Ti atoms substitute Zn in the hexagonal lattice and Ti ions may occupy the interstitial sites of ZnO or probably Ti segregates to the non-crystalline region in grain boundaries and forms Ti-O bond. From Fig.1, it can be noticed that the intensity of (002) peak ($I_{(002)}$) is much stronger than the others. Corresponding to the Ti-doping contents of 0%, 2%, 3% and 5%, the $I_{(002)}$ values are found from Tab.1 to be 6.305 3×10^4, 2.868 2×10^5, 1.596 7×10^6 and 9.009 0×10^5 cycles per second, respectively. Obviously, the $I_{(002)}$ is observed to increase initially and then decrease with the increase of the Ti-doping content. The degree of preferred (002) orientation ($P_{(002)}$) of the thin films can be defined as[12]:

$$P_{(002)} = \frac{I_{(002)}}{I_{(100)} + I_{(002)} + I_{(110)}} \times 100\% , \quad (1)$$

where $I_{(100)}$, $I_{(002)}$ and $I_{(101)}$ are the intensities of (100), (002) and (101) diffraction peaks, respectively. The degrees of preferred (002) orientation $P_{(002)}$ can be calculated using Eq.(1) to be 88.81%, 99.83%, 99.87% and 99.81% for the Ti-ZnO samples with Ti-doping contents of 0%, 2%, 3% and 5%, respectively. Clearly, all the deposited films present (002) plane as the preferred orientation. This (002) preferred orientation is due to the fact that the most densely packed (002) plane in wurtzite ZnO has the lowest surface free energy[16]. The results indicate that the deposited films are single phased with a hexagonal structure characteristic of pure ZnO. All the samples exhibit preferential orientation with c-axis perpendicular to the substrate surface.

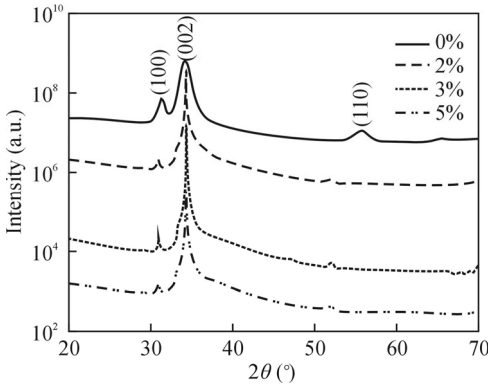

Fig.1 XRD patterns of ZnO and Ti-ZnO thin films

Tab.1 The XRD analysis results of the deposited thin films

Content (%)	$I_{(002)}$ (cycles per second)	$P_{(002)}$ (%)	*FWHM* (°)	*D* (nm)	ε
0	6.305 3×10^4	88.81	0.785	10.6	4.939×10^{-3}
2	2.868 2×10^5	99.83	0.112	74.2	7.063×10^{-4}
3	1.596 7×10^6	99.87	0.101	83.2	6.263×10^{-4}
5	9.009 0×10^5	99.81	0.136	61.1	8.529×10^{-4}

From Tab.1, we note that the full width at half maximum (*FWHM*) of (002) peak for the deposited films decreases significantly with the Ti-doping content up to 3%, and then it increases slightly above 3%. The decrease of the *FWHM* indicates the increase of crystallite size of the thin films. The crystallite size (*D*) is evaluated according to the well-known Scherrer's formula[17] as follows:

$$D = \frac{0.90 \cdot \lambda}{FWHM \cdot \cos\theta} , \quad (2)$$

where λ is the wavelength of used X-rays (λ=0.154 06 nm), θ is the Bragg's diffraction angle and *FWHM* is the full width at half maximum in radians of the (002) diffraction peak. The lattice strain (ε) can be estimated using the following relation[18]:

$$\varepsilon = \frac{\lambda}{D \cdot \sin\theta} - \frac{FWHM}{\tan\theta} . \quad (3)$$

The values of *FWHM* and θ from the XRD peaks are estimated by Gaussian fitting. The values of *D* and ε for ZnO and Ti-ZnO samples with different Ti-doping contents are calculated and listed in Tab.1. The crystallite size is found to be in the range of 10.6—83.2 nm with the Ti-doping content ranging from 0% to 5%, and reaches the highest value of 83.2 nm at the Ti-doping content of 3%. From Tab.1, the change tendency of the lattice strain is observed to be opposite to the crystallite size. Obviously, the Ti-ZnO sample prepared with the Ti-doping content of 3% possesses the best crystal quality, with the minimum *FWHM* of 0.101°, the maximum *D* of 83.2 nm and the lowest ε of 6.263×10^{-4}. The results suggest that the crystalline quality of the

Ti-ZnO thin films depends on the Ti-doping content significantly.

Fig.2 displays the optical transmittance (T) of ZnO and Ti-ZnO samples with different Ti-doping contents. As can be seen, all the samples have high transparency in the visible region. Also, all the transmittance curves exhibit oscillations due to the interference effect of light between two interfaces of the air/film and film/substrate, indicating that these thin films have low surface roughness and good homogeneity. The average optical transmittance (T_{av}) in the visible range exceeds 84.5% for all the deposited films, as shown in the inset of Fig.2. The T_{av} increases with the increase of Ti-doping content up to 3%, reaches the maximum of 88.8%, and then decreases to 86.4% at Ti-doping content of 5%. The highest T_{av} of 88.8% is obtained at the Ti-doping content of 3%.

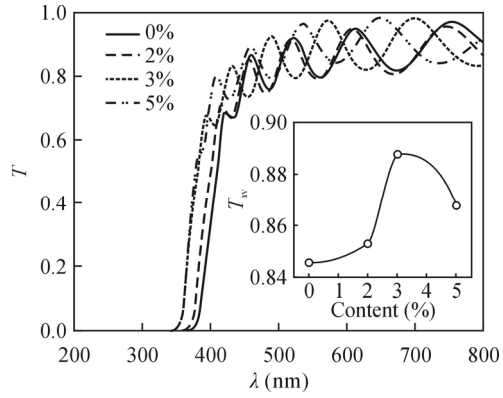

Fig.2 Optical transmittance spectra of ZnO and Ti-ZnO thin films

Fig.3(a) presents the electrical resistivities (ρ) of ZnO and Ti-ZnO samples with different Ti-doping contents. As the Ti-doping content increases from 0% to 5%, the ρ decreases firstly and then increases. The minimal ρ of 1.18×10^{-3} Ω·cm is obtained for the sample prepared with the Ti-doping content of 3%. The decrease of resistivity can be attributed to the improvement of crystallinity and the increase of crystallite size, which is confirmed by the results of XRD discussed above. In order to quantify the optoelectronic performance of the deposited TCO thin films, the figure of merit (*FOM*) is introduced and defined as[19]:

$$FOM = \frac{1}{\rho \ln\left(1/T_{av}\right)}, \tag{4}$$

where T_{av} is the average transmittance in the visible range and ρ is the resistivity of the thin films. The higher the figure of merit, the better the performance of the TCO thin films. Fig.3(b) shows the variation of *FOM* values for the samples prepared with different Ti-doping contents. The *FOM* is found to rise initially and then fall with the increment of the Ti-doping content. With the best combination of high transmission and low resistivity, the highest *FOM* of 7.08×10^{3} $\Omega^{-1}\cdot cm^{-1}$ is obtained at Ti-doping content of 3%. This high *FOM* for the Ti-ZnO thin films implies that they are suitable for transparent contacts in various optoelectronic devices.

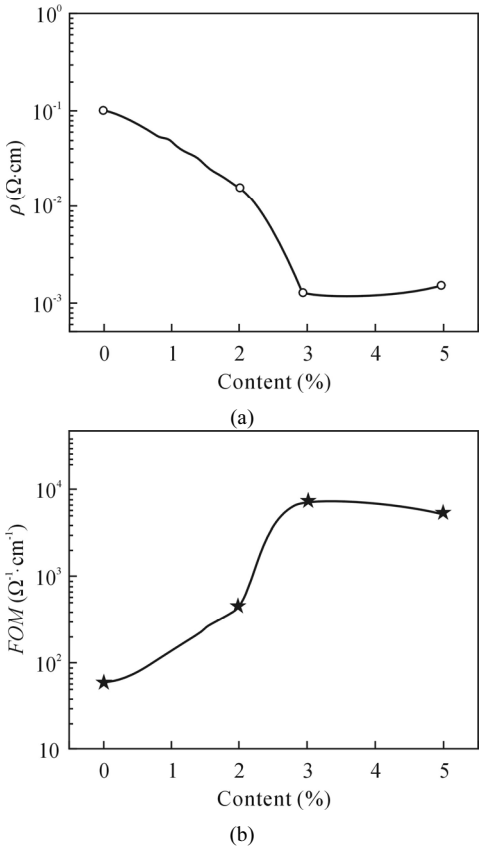

Fig.3 (a) Resistivity and (b) figure of merit for ZnO and Ti-ZnO thin films

The band edge of the films is estimated using the relation where the absorption coefficient (α) is a parabolic function of the incident photon energy (E) and the optical bandgap (E_g), i.e.,

$$(\alpha \cdot E)^2 = C\left(E - E_g\right), \tag{5}$$

where C is an energy-independent constant. Using Eq.(5), the bandgap edge of the deposited film is evaluated by plotting $(\alpha E)^2$ as a function of the energy E of the incident radiation, and extrapolating the linear part of the curve to intercept the energy axis[20]. Fig.4 shows the Tauc's plots of $(\alpha E)^2$ versus E for all the samples. The obtained optical bandgaps are found to be about 3.319 eV, 3.453 eV and 3.465 eV for the Ti-ZnO samples with Ti-doping contents of 2%, 3% and 5%, respectively. These E_g values are larger than that of undoped ZnO (about 3.237 eV), which is due to the Burstein-Moss (B-M) effect[21,22].

In conclusion, transparent conducting Ti-ZnO nanostructured thin films were prepared by RF magnetron sputtering, and the effects of the Ti-doping content on the structural and optoelectronic properties of the thin

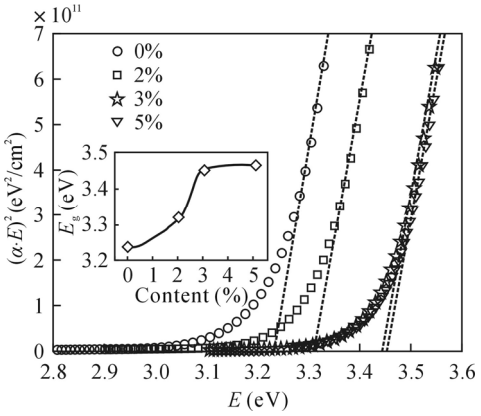

Fig.4 Plots of $(\alpha E)^2$-E for ZnO and Ti-ZnO thin films

films are investigated. It is observed that all the deposited films are of polycrystalline nature. The Ti-ZnO thin film deposited with the Ti-doping content of 3% exhibits the best crystallinity and optoelectronic properties, which has the highest degree of preferred (002) orientation of 99.87%, the maximum crystallite size of 83.2 nm, the minimum lattice strain of 6.263×10^{-4}, the highest average visible transmittance of 88.8%, the lowest electrical resistivity of 1.18×10^{-3} Ω·cm and the highest figure of merit of 7.08×10^{3} $\Omega^{-1}\cdot cm^{-1}$. The optical bandgaps of the deposited films are estimated by Tauc's law. A blue shift of the optical bandgap is observed with an increase of the Ti-doping content.

References

[1] Song Y S, Seong N J, Choi K J and Ryu S O, Thin Solid Films **546**, 271 (2013).

[2] Zhang Qiang, Qin Wen-jing, Cao Huan-qi, Yang Li-ying, Zhang Feng-ling and Yin Shou-gen, Optoelectron. Lett. **10**, 0253 (2014).

[3] Ma Q-B, Ye Z-Z, He H-P, Zhu L-P and Zhao B-H, Mater. Sci. Semicond. Process. **10**, 167 (2007).

[4] Du Shuai, Zhang Fang-hui, Cheng Jun and Li Huai-kun, J. Optoelectron. Laser **26**, 1878 (2015). (in Chinese)

[5] Chen Zheng and Deng Zhen-bo, Optoelectron. Lett. **11**, 0187 (2015).

[6] Yamamoto N, Makino H, Osone S, Ujihara A, Ito T, Hokari H, Maruyama T and Yamamoto T, Thin Solid Films **520**, 4131 (2012).

[7] Wu J-L, Lin H-Y, Su B-Y, Chen Y-C, Chu S-Y, Liu S-Y, Chang Ch-C and Wu C-J, J. Alloy Compd. **592**, 35 (2014).

[8] Hjiri M, El Mir L, Leonardi S G, Pistone A, Mavilia L and Neri G, Sensor Actuat. B **196**, 413 (2014).

[9] Chen X-L, Wang F, Geng X-H, Zhang D-K, Wei C-C, Zhang X-D and Zhao Y, Appl. Surf. Sci. **258**, 4092 (2012).

[10] Ye Yun, Cai Shou-jin, Yan Min, Chen Tian-yuan, Liu Yu-hui, Guo Tai-liang and Lin Zhi-xian, J. Optoelectron. Laser **25**, 101 (2014). (in Chinese)

[11] Chen Shoubu and Wei Shiliang, J. South-Cent. Univ. Nationlities (Nat. Sci. Ed.) **34**, 72 (2015). (in Chinese)

[12] Chen J, Chen D, He J, Zhang S and Chen Z, Appl. Surf .Sci. **255**, 9413 (2009).

[13] Yu Xuan, Yu Xiao-ming, Zhang Jian-jun and Pan Hong-jun, Optoelectron. Lett. **11**, 0329 (2015).

[14] Rozati S M and Akeste S, Cryst. Res. Technol. **43**, 273 (2008).

[15] Zou Y S, Yang H, Wang H P, Lou D, Tu C J and Zhang Y C, Phys. B **414**, 7 (2013).

[16] Jin B J, Bae S H, Lee S Y and Im S, Mater. Sci. Eng. B **71**, 301 (2000).

[17] Huang T, Li C, Wu J, Zhou Z, Chi Q and Liu H, J. South-Cent. Univ. Nationlities (Nat. Sci. Ed.) **32**, 5 (2013). (in Chinese)

[18] Klug P and Alexander L E, X-Ray Diffraction Procedures for Polycrystalline and Amorphous Materials, New York: Wiley, 1974.

[19] Cho S, Microelectron. Eng. **89**, 84 (2012).

[20] Gu J, Zhong Z, He X and Sun F, J. South-Cent. Univ. Nationlities (Nat. Sci. Ed.) **28**, 30 (2009). (in Chinese)

[21] Zi Xing-fa, Ye Qing, Liu Rui-ming and He Yong-tai, J. Optoelectron. Laser **26**, 883 (2015). (in Chinese)

[22] Ben Ayadi Z, El Mir L, Djessas K and Alaya S, Mater. Sci. Eng. C **28**, 613 (2008).